Submitted to ADVANCED FUNCTIONAL MATERIALS

DOI: 10.1002/adfm.((please insert DOI)

Very High Efficiency Orange-Red Light-Emitting Devices with Low Roll-Off at High Luminance Based on an Ideal Host-Guest System Consisting of Two Novel Phosphorescent Iridium Complexes with Bipolar Transport

By *Guomeng Li, Dongxia Zhu, Tai Peng, Yu Liu,* Yue Wang,* and Martin R. Bryce**

((Optional Dedication))

[*]Prof. Y. Liu, Y. Wang, Dr. G. Li, T. Peng
State Key Laboratory of Supramolecular Structure and Materials
College of Chemistry, Jilin University, Changchun 130012 (P. R. China)
E-mail: yuliu@jlu.edu.cn, yuewang@jlu.edu.cn

Prof. D. Zhu
Institute of Functional Material Chemistry, Faculty of Chemistry, Northeast Normal University, Renmin Road 5268, Changchun, Jilin 130024 P. R. China

[*]Prof. M. R. Bryce
Department of Chemistry, Durham University, Durham, DH1 3LE, UK
E-mail: m.r.bryce@durham.ac.uk

Keywords: Electrophosphorescence • Bipolar Transporting Property • All-phosphor Doping System • Iridium Complex • Organic Light-emitting Device

Abstract: Two phosphorescent iridium complexes with bipolar transporting ability, namely FPPCA (500 nm) and BZQPG (600 nm), have been synthesized and employed as an ideal host-guest system for phosphorescent organic light emitting diodes (PHOLEDs).The devices give very high-efficiency orange-red emission from BZQPG with maximum external quantum efficiency (EQE or η_{ext}) of >27% and maximum power efficiency (PE or η_p) of >75 lm/W, and maintain high levels of 26% and 55 lm/W, 25% and 40 lm/W at high luminance of 1000 and 5000 cd m^{-2}, respectively, within a range of 8-15 wt% of BZQPG. The realization of such high and stable EL performance results from the coexistence of two parallel paths: (i) effective energy transfer from host (FPPCA) to guest (BZQPG) and (ii) direct exciton formation on the BZQPG emitter, which can alternately dominate the electrophosphorescent emission. This all-phosphor doping system removes the charge-injection barrier from the charge-transport process to the emissive layer (EML) due to the inherent narrow Eg of both phosphors. Therefore, this ideal host-guest system represents a new design to produce

PHOLEDs with high efficiency and low efficiency roll-off using a simple device configuration.

1. Introduction

Orange-red or red electrophosphorescent emitters are very important in order to achieve highly efficient fluorescence-phosphorescence hybrid or all phosphor-doped full color displays and white organic light-emitting devices (OLEDs) with high color rendering index (CRI) values (>80).[1] Recently, significant progress has been made in red or orange-red or orange electroluminescent (EL) devices with the external quantum efficiency of ≈25%.[2] Nevertheless, among them, the EL performances of the true orange-red or red devices that meet the standard of $\lambda_{max}^{EL} \geq 580$ nm and/or the Commission Internationale de L'Eclairage ($CIE_{x,y}$) coordinates of $x \geq 0.55$ and $y \leq 0.45$, [2b,c,e] are still far from satisfactory due to their moderate power efficiency (<50 lm/W) and significant efficiency roll-off. Generally, there are two main factors causing the efficiency roll-off at high luminance: (i) large energy gaps (E_g) between the HOMO (highest occupied molecular orbital) and LUMO (lowest unoccupied molecular orbital) levels associated with their high triplet energies, and (ii) loss of charge balance in the organic host matrix.[3] These factors result in inefficient charge carrier injection, leading to a high driving voltage. Additionally, narrow charge aggregation and recombination zones which are close to the interface between the emission layer (EML) and the electron transport layer (ETL) or hole transport layer (HTL) increase the probability of triplet-triplet annihilation (TTA) which will reduce EL efficiencies, especially at high luminance levels. Thus, it is highly desirable to develop new host-guest systems for enhanced orange or orange-red emission in phosphorescent organic light-emitting diodes (PHOLEDs). The host should have: (i) a higher triplet energy than the guest, (ii) a relatively narrow E_g and well-matched HOMO/LUMO levels with the HTL/ETL and (iii) high and well-balanced carrier-transport

properties. Phosphorescent iridium complexes could meet these criteria, although research on this topic has been rather limited.[3a,4]

We now report two novel iridium complexes $(F_2ppy)_2Ir(dipcca)$ (FPPCA) and $(bzq)_2Ir(dipig)$ (BZQPG) with green (~500 nm) and orange-red (~600 nm) electroluminescence, which act as host and guest emitters, respectively. Both of the phosphors possess sufficient and balanced hole and electron mobilities (~10^{-3} cm^2 V^{-1} s^{-1}). This ensures that both charge carrier species smoothly conduct by hopping between the adjacent host and guest molecules within the EML. As a result, two emission mechanisms co-exist in the EML: namely (i) complete energy transfer from green (host) to orange-red phosphor (guest) and (ii) direct exciton formation on the guest emitter.[5] We have fabricated orange-red PHOLEDs (λ_{max}^{EL}~590 nm) with very high external quantum efficiency (EQE) and PE, and low efficiency roll-off at high luminance levels. At 8% and 15% dopant concentration constant Commission Internationale de L'Eclairage ($CIE_{x,y}$) coordinates of (0.57±0.01, 0.41±0.01) and comparable $\eta_{ext,\,max}$ of 27.9, 26.3% and $\eta_{p,\,max}$ of 76.8, 77.5 lm/W respectively, were obtained. High levels of 26% / 55 lm/W, and 25% / 40 lm/W were retained at high luminance of 1000 and 5000 cd m^{-2}. To the best of our knowledge, all the EL efficiency values above are significantly higher than previously reported for orange devices with similar CIE coordinates (see the reference data in the bottom two rows of **Table 1**). One report uses a complicated EML comprising four co-doped components including an exciplex-forming host (the molar ratio of TCTA to B3PYMPM is 1:1) doped with both a green (8 wt%) and a red Ir complex (0.5 wt%) in precise concentrations.[2c] Another leading report[2d] demonstrates very high efficiencies and low roll-off using a bipolar host and an Ir phosphor guest, however, the PHOLEDs have more yellow-orange emission ($CIE_{x,y}$ 0.51, 0.49) than the present work, and therefore the data are not directly comparable. Efficient yellow / yellow-orange emission (CIE_x 0.48-0.49; CIE_y 0.50-0.51) is also observed in other recent work.[2i] It is obviously

desirable that the EL performance is independent of the doping concentration within a certain range, as is the case in our devices. This leads to an easily controlled process for fabricating highly efficient PHOLEDs, although the current high cost of iridium may limit large-scale commercial production.

2. Results and Discussion

2.1. Synthesis and Photophysical Properties

The new complexes FPPCA and BZQPG were synthesized in high yields following precedents for analogs[6] (see the Supporting Information). Their structures (see **Figure 1a**) and purity were confirmed by ^{1}H NMR spectroscopy, mass spectrometry and elemental analysis. An unusual feature of the complexes is their bipolar properties. This is achieved by attaching electron donating substituents onto the N^N amidinate ligands, combined with electron-withdrawing C^N ligands. Their UV/Vis absorption and photoluminescence (PL) spectra in neat and doped thin films are shown in **Figure 1b**. The neat BZQPG film shows strong orange-red PL emission at λ_{max} 605 nm with a quantum yield of 0.26±0.02 and FPPCA film shows green emission at λ_{max} 500 nm, with a quantum yield of 0.35±0.02. The corresponding triplet energies (T_1) were estimated to be BZQPG ~2.1 eV (λ=605 nm) and FPPCA ~2.4 eV (λ=500 nm) from the 0−0 band of their phosphorescence spectra. Therefore, the triplet energy alignment, together with a large overlap between the phosphorescence spectrum of FPPCA (λ=500 nm) and the MLCT absorption band of BZQPG (475-550 nm), suggests efficient triplet energy transfer from FPPCA (host) to BZQPG (guest). This has been demonstrated in the PL spectra of doped FPPCA:BZQPG thin film with 8 wt% of BZQPG which shows emission only from BZQPG (**Figure 1b)**. The short phosphorescence lifetimes of FPPCA and BZQPG in toluene solution, 0.08 and 0.14 μs, respectively, suggest that efficient spin−orbit coupling leads to intersystem crossing from the singlet to triplet states in

each complex. Short lifetimes are beneficial for increasing spin-state mixing and reducing the roll-off in electroluminescent (EL) efficiency.[7]

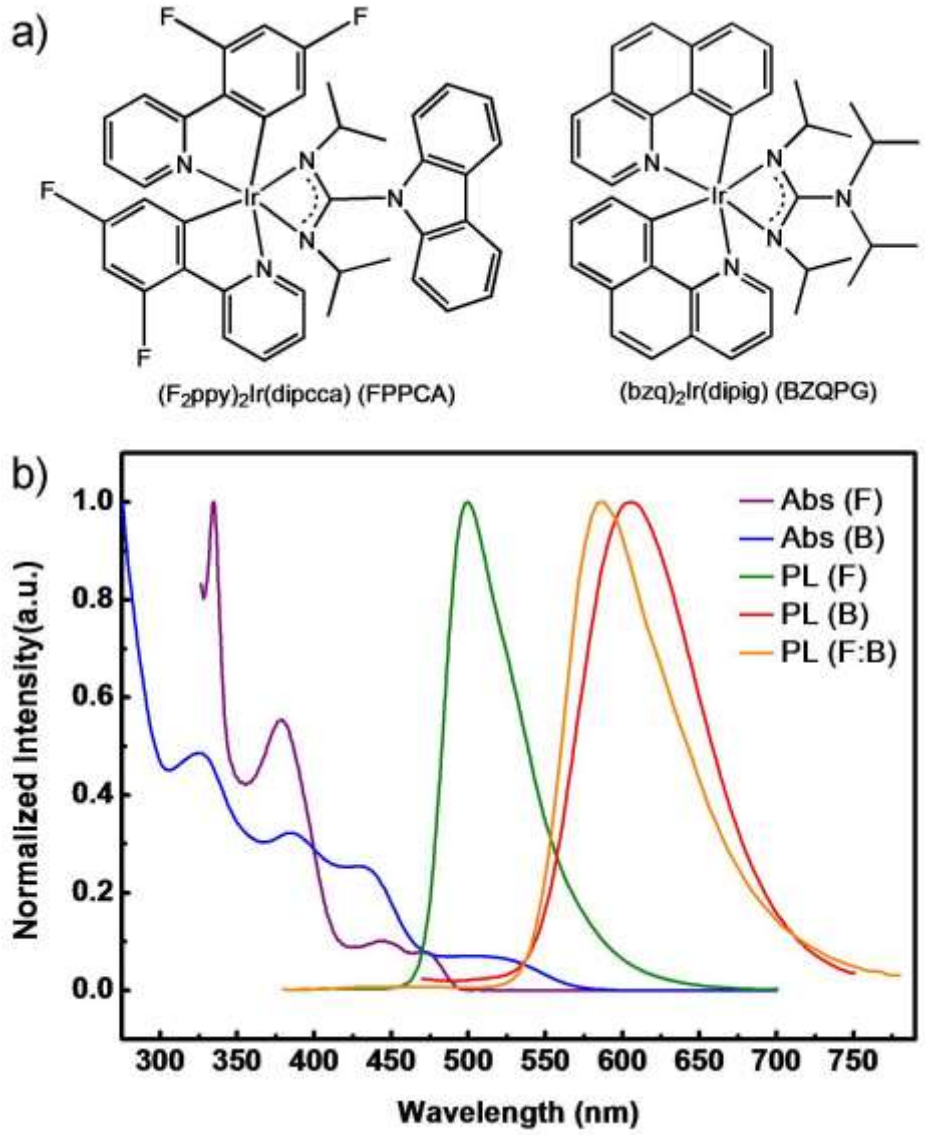

Figure 1. a) Molecular structures of FPPCA and BZQPG. b) UV-Vis absorption and PL spectra of FPPCA (F) and BZQPG (B) in neat thin film, and PL spectrum of BZQPG doped in FPPCA thin films with 8 wt% doping concentration.

2.2. Energy-Level Property and Time-Of-Flight (TOF) Measurement

As shown in **Figure 2a**, the HOMO/LUMO levels of FPPCA (-5.3/-2.8 eV) and BZQPG (-4.9/-2.7 eV) are well matched with those of common charge transport materials: 4,4′-bis(*N*-(1-naphthyl)-*N*-phenylamino)biphenyl (NPB) for holes and 1,3,5-tris(*N*-phenylbenzimidazol-2-

yl)benzene (TPBI) for electrons, which will be used in PHOLEDs below. Thus the HOMO/LUMO levels of FPPCA and BZQPG are more suitable for both hole and electron injection into the EML compared with the usual fluorescent host materials, such as 4,4′-*N*,*N*'-dicarbazolylbiphenyl (CBP). Time-of-flight (TOF) measurements (**Figure 3**) revealed that the hole and electron mobilities of FPPCA and BZQPG are 5.9×10^{-3} and 6.3×10^{-3} cm^2 V^{-1} s^{-1}, and 2.9×10^{-3} and 2.3×10^{-3} cm^2 V^{-1} s^{-1}, respectively. The measurements were made at an electric field of 5.0×10^{-5} V cm^{-1} at 293 K in vacuum. These are rather high mobility values for phosphorescent emitters, and are similar to, or much higher than, the values obtained for typical charge transport materials including NPB (3.9×10^{-4} cm^2 V^{-1} s^{-1}) and TPBI (9.6×10^{-6} cm^2 V^{-1} s^{-1}) measured under the same experimental conditions. Literature values for NPB are ~10^{-4} cm^2 V^{-1} s^{-1}[8] and for TPBI are ~10^{-5} cm^2 V^{-1} s^{-1}.[9] Therefore, high recombination efficiency of holes and electrons is expected based on direct charge injection into, and balanced transport within, the EML through the bipolar FPPCA and BZQPG molecules.

2.3. PHOLEDs Design and Performance

To explore the EL performance of this all-phosphor host-guest system, six PHOLEDs were fabricated with the device structures shown in **Figure 2b**. In each device, NPB served as the hole-transport layer (HTL) and TPBI as the electron-transport layer (ETL), with ITO (indium-tin oxide) anode and LiF/Al cathode. The devices using neat FPPCA film, doped FPPCA : BZQPG (8 wt% and 15 wt% BZQPG) films, and neat BZQPG film are denoted as PIr100, PIr8, PIr15 and Ir100, respectively. For comparison, two devices (CIr8 and CIr15) with the same configurations as the devices PIr8 and PIr15, respectively, were fabricated by using CBP as the host instead of FPPCA. Both NPB and TPBI possess “mono-polar” carrier transporting properties,[10] and they have a wider energy gap than FPPCA and BZQPG, as

shown in **Figure 2a**. Therefore, the EML based on neat FPPCA, neat BZQPG or doped FPPCA: BZQPG films is the expected zone for exciton generation and recombination without introducing other barrier layers. A key to maximizing the EL efficiency of these devices is the facile inter-zone injection of both holes and electrons onto the emitters due to the cascaded energy level diagram. The bipolar charge transport ability of FPPCA and BZQPG will effectively eliminate the accumulated carriers, resulting in balanced and sufficient charge fluxes within the EMLs. The comparable hole-only and electron-only data in single-carrier devices for both complexes are shown in the Supporting Information (Figures SI-4 and SI-5). This will lead to the exciton recombination regions being broadened as wide as the entire EML.[3c,11] These favorable factors are expected to significantly reduce the triplet-triplet annihilation (TTA) process in the EMLs and thus achieve very high EL efficiency, together with low roll-off at high luminance/current density levels.

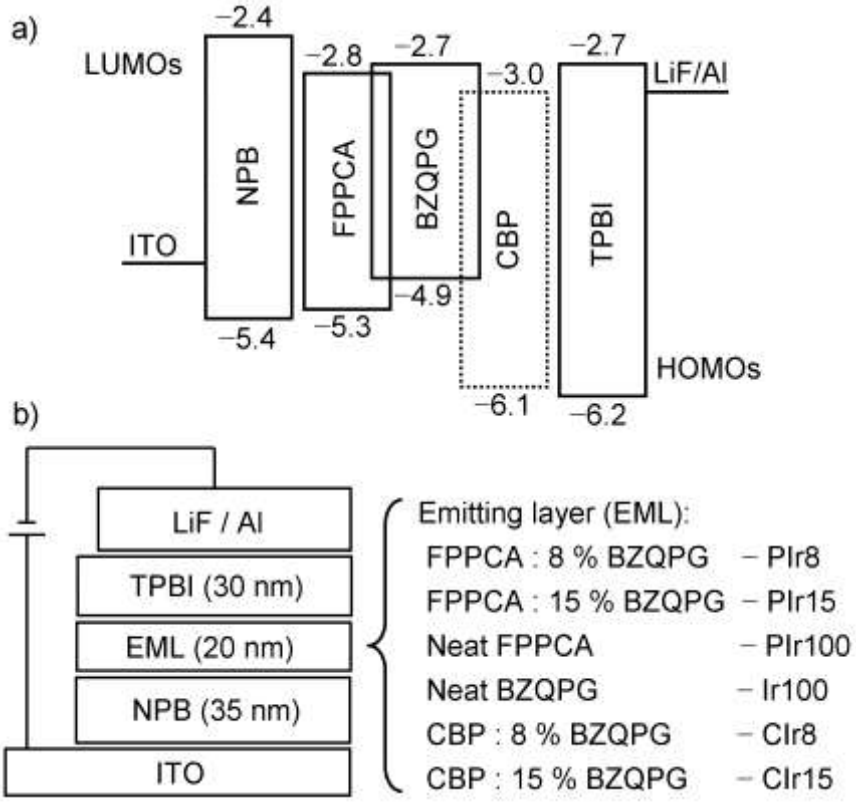

Figure 2. a) Proposed energy diagram of the materials used in OLEDs. b) Schematic structures of the devices PIr8, PIr15, PIr100, Ir100, CIr8 and CIr15.

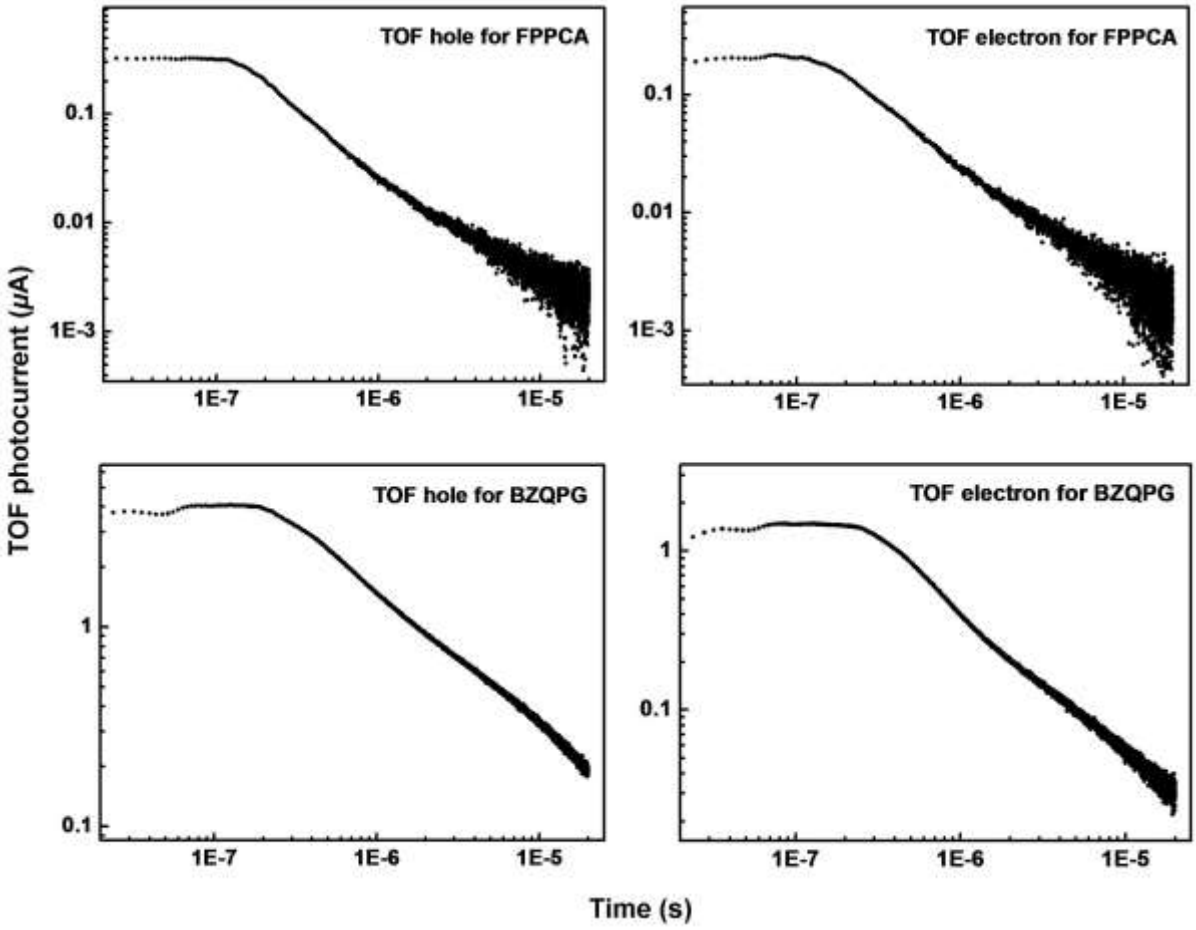

Figure 3. Time-of-flight transients for hole and electron mobilities for FPPCA and BZQPG.

Figure 4 shows the EL spectra of all the devices at luminance 10000 cd m^{-2}. PIr100 presents bright green phosphorescent emission, which is identical to the PL spectrum of neat FPPCA film (**Figure 1**). The other devices exhibit strong orange-red emission from BZQPG with λ_{max}^{EL} 588-600 nm and ($CIE_{x,y}$) coordinates of (0.57±0.01, 0.41±0.01). No host emission is observed in the EL spectra of the doped devices. This confirms that complete energy transfer occurs from FPPCA or CBP to BZQPG at a dopant concentration of ≥8 wt%. The current density-voltage-luminance (*J-V-L*) and EL efficiency-luminance (PE/EQE-*L*) characteristics are shown in **Figures 5a** and **5b**. The data are summarized in **Table 1**, along with comparative data for the current state-of-the-art PHOLEDs with similar CIE coordinates to our devices.[2c,2d] Devices PIr100, PIr8, PIr15 and Ir100 displayed low driving voltages

based on the rapidly increasing *J-V* and *L-V* curves after the onset. The turn-on voltages (V_{on} at 1 cd m^{-2}) of PIr100, PIr8, PIr15 and Ir100 are as low as 2.4, 2.4, 2.3 and 2.2 V. The driving voltages at the practical luminance of 1000 cd m^{-2} are 3.5 V, 4.2, and 3.7 V and 4.1 V, respectively. At driving voltages of 4.4, 5.3, 4.8 and 5.7 V for PIr100, PIr8, PIr15 and Ir100, very high luminances of >5000 cd m^{-2} were obtained. In contrast, the driving voltages of reference devices CIr8 and CIr15, based on CBP host, increased with different degrees, depending on the BZQPG concentration. The turn-on (1 cd m^{-2}) and driving voltages (1000 and 5000 cd m^{-2}) for CIr8 are 3.3, 5.7 and 7.5 V; for CIr15 they are 2.5, 4.7 and 6.1 V, respectively. The driving voltages of PIr100, PIr8, PIr15 and Ir100 at the current density of 1 and 10 (in brackets) mA/cm^2 are 3.3 (4.5), 4.1 (5.7), 3.5 (5.1) and 3.1 (4.3) V, which are significantly lower than 5.1 (6.9) and 4.4 (6.1) V for CIr8 and CIr15 at the corresponding current density levels. The much lower driving voltages of the devices without CBP, and the reduced driving voltages with increasing the doping concentration of BZQPG in the devices CIr8 and CIr15, are explained by the direct charge injection/transport through the FPPCA and BZQPG complexes followed by exciton formation on both of the phosphors. We note that with an optimized device structure high efficiencies for yellow-orange PHOLEDs without satisfactory bipolar carrier mobility can be obtained using CPB host at higher driving voltages.[2i]

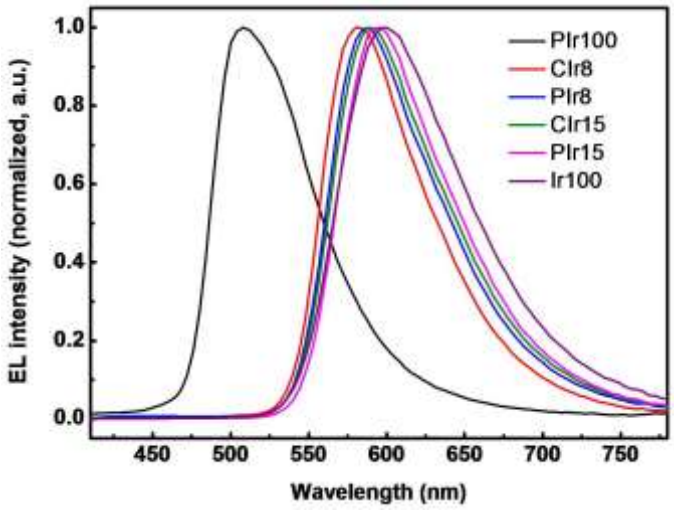

Figure 4. EL spectra of PIr100, PIr8, PIr15, CIr8, CIr15 and Ir100 at the luminance of 10000 cd m^{-2}.

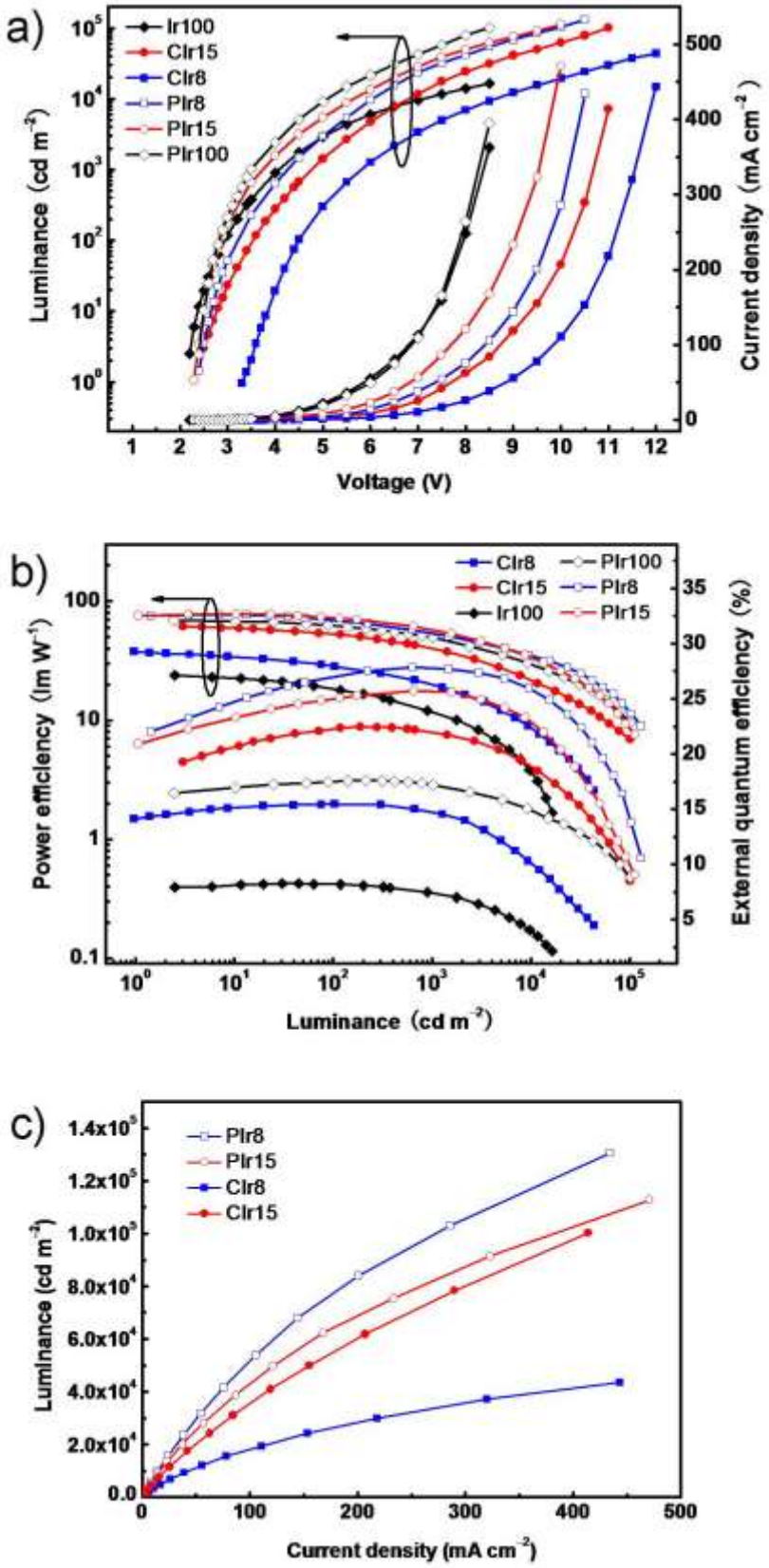

Figure 5. a) Current density-voltage-luminance (*J-V-L*) curves of PIr100, PIr8, PIr15, CIr8, CIr15 and Ir100. b) Power efficiency-luminance-external quantum efficiency curves of PIr100, PIr8, PIr15, CIr8, CIr15 and Ir100. c) Luminance-current density (*L-J*) curves of PIr8, PIr15, CIr8 and CIr15.

Table 1. EL data of devices PIr100, PIr8, PIr15, CIr8, CIr15, Ir100 and current state-of-the-art literature data for orange PHOLEDs.

Device	V_{on} [a)] [V]	V [b)] [V]	L_{max} [cd m^{-2}] (V at L_{max})	CIE (x,y) [c)]	$\eta_{p.max}$ [lm W^{-1}]	$\eta_{ext.max}$ [%]	η_p [b)] [lm W^{-1}]	η_{ext} [d)] [%]
PIr100	2.4	3.5, 4.4	100950 (8.5)	0.27,0.58	68.8	17.6	49.3, 35.5	15.8, 14.3
PIr8	2.4	4.2, 5.3	130500 (10.5)	0.57,0.42	76.8	27.9	55.6, 41.5	26.5, 24.3
CIr8	3.3	5.7, 7.5	43610 (12)	0.56,0.42	37.6	15.5	19.9, 12.1	13.2, 11.1
PIr15	2.3	3.7, 4.8	112750 (10)	0.58,0.41	77.5	26.3	58.7, 42.3	24.6, 22.1
CIr15	2.5	4.7, 6.1	91030 (11)	0.57,0.41	61.5	22.5	40.6, 27.5	20.1, 18.2
Ir100	2.2	4.1, 5.7	16350 (8.5)	0.58,0.40	23.8	8.3	11.7, 6.5	7.3, 6.1
Ref.[2c] [e)]	2.4	~3.8, 4.2	--	0.55,0.43	49.5	25.4	39.1, 30.0	23.3, 21.1
Ref.[2d] [f)]	2.75	3.96, --	--	(0.51,0.49)	64.5	24.5	57.3, --	24.2, --

[a)] Applied voltage required to reach a luminance of 1 cd m^{-2}. [b)] Values at 1000 and 5000 cd m^{-2}, respectively. [c)] Recorded at 10000 cd m^{-2}. [d)] Values at 10 and 30 mA cm^{-2}, respectively. [e)] Highest literature efficiency values for a PHOLED with similar CIE coordinates. The device is based on a EML containing four co-doped components including an exciplex-forming (the molar ratio of TCTA to B3PYMPM is 1:1) host doped with both a green (8 wt%) and a red (0.5 wt%) Ir phosphor.[2c] [f)] The device is based on a bipolar indolocarbazole/1, 3, 5-triazine host molecule and a yellow-orange Ir phosphor dopant. [2d]

The PIr100 and Ir100 devices, based on the neat FPPCA or BZQPG EML, showed the highest EL efficiency for non-doped green and orange-red PHOLEDs with the maximum PE of 68.8, 23.8 lm W^{-1}, and EQE of 17.6, 8.3%,[6, 12] respectively. The roll-off of the EQE is very low with values of 17.2 and 7.4% at 1000 cd m^{-2} (**Figure 5b**). The high-efficiency green and orange-red electrophosphorescence is evidence for direct exciton formation on the FPPCA (PIr100) or BZQPG (Ir100) complexes: this is the only possible mechanism for EL from the neat EMLs without a host. This occurs due to the exceptional multifunctional character of both phosphors, including their balanced charge transport, high quantum yield in the solid state and short excited state lifetimes. For the doped-EML system: i.e. the PIr8 and PIr15 devices with doped FPPCA:BZQPG EMLs, and CIr8 and CIr15 with doped CBP:BZQPG EMLs, the EL emission from BZQPG should be achieved through two

complementary mechanisms. These mechanisms are: (i) direct exciton formation on the BZQPG molecules and (ii) complete triplet excited state energy transfer from FPPCA or CBP to the guest BZQPG. Due to the similar energy level characteristics and virtually identical charge-transporting properties of FPPCA and BZQPG, their different ratios in the EMLs have only a minimal effect on exciton formation in PIr8 and PIr15. This is confirmed by the comparable EL characteristics of both devices shown in **Figure 5b** and **Table 1**. As the most highly efficient orange-red OLEDs, PIr8 and PIr15 possess maximum PE and EQE values of 76.8, 77.5 lm W^{-1} and 27.9, 26.3%, respectively. To the best of our knowledge, these EL efficiencies exceed any previously reported values for orange-red OLEDs with similar CIE coordinates.[2c,2j] Moreover, the efficiency roll-off of PIr8 and PIr15 is low upon increasing the luminance and current density. The PE and EQE of PIr8 and PIr15 at a practical luminance of 1000 cd m^{-2} maintained the very high levels of 55.6, 58.7 lm W^{-1} and 27.8, 26.2%, respectively. Moreover, >90% of the maximum EQE is maintained up to the extremely high luminance of 10000 cd m^{-2}. Furthermore, the EQE values remain >20% over the very wide luminance range of 1–50000 cd m^{-2} for PIr8 and 1–25000 cd m^{-2} for PIr15, corresponding to wide current density ranges of ca. 0.001–100 mA cm^{-2} for PIr8 and 0.001–50 mA cm^{-2} for PIr15. These ultra-high efficiencies and remarkably low roll-off are competitive with the best reported PHOLEDs.[13] These data demonstrate that TTA processes, especially at high luminance levels, have been greatly reduced. This results from the balanced charge fluxes and broader recombination zones within the EMLs of PIr8 and PIr15 due to the bipolar and comparable charge transporting ability of FPPCA and BZQPG complexes. Nevertheless, it can be seen from **Figure 5b** that PIr15 showed slightly lower EQE and higher roll-off than PIr8. This implies slightly more TTA quenching in PIr15 than in PIr8, which is supported by the lower luminance of PIr15 than of PIr8 at a constant current density (**Figure 5c**). In PIr8, the optimal content of BZQPG ensures that two simultaneous processes of direct

exciton formation on BZQPG and triplet energy transfer from FPPCA to BZQPG combine to harvest all the excitons, and achieve the high emission efficiency. At the same current density, the higher content of BZQPG in PIr15 results in excess triplet formation directly on the guest molecules, leading to increased TTA and thus decreased luminance and EQE values.

In contrast, CIr8 and CIr15 showed significantly lower PE and EQE than PIr8 and PIr15. The EL efficiencies of CIr8 and CIr15 are very dependent on BZQPG content (**Figure 5b**). For instance, CIr8 and CIr15 showed maximum PE of 37.6, 61.5 lm W^{-1}, and EQEs of 15.5, 22.5%. The roll-off for these devices is significant with PEs of 19.9, 40.6 lm W^{-1} and EQEs of 14.8, 21.8% at 1000 cd m^{-2}, respectively. The dependence of EL efficiency shown here, together with the consistent *J-V-L* characteristics of CIr8 and CIr15 (**Figure 5a**) and the single-carrier devices (**Figure S5** in the Supporting Information), further confirm that in the EMLs of CBP-host devices, the BZQPG molecules provide a more favorable charge-transport channel than the CBP molecules. This is due to the narrower energy gap and more balanced charge-transport ability of BZQPG than of CBP. Hence, increasing BZQPG concentration will improve the charge injection into the EML and reduce the hopping distance between neighboring BZQPG molecules. This will further enhance the charge conduction and lead to more excitons directly generated in the EML; this explains the considerably higher luminance of CIr15 compared to CIr8 in **Figure 5c**. Furthermore, as seen in **Figure 4c**, at a fixed concentration of 8 wt% BZQPG, where the primary emission mechanism is energy transfer due to the low content of BZQPG, the more rapidly rising luminance curve of PIr8 compared to CIr8 indicates that FPPCA is a more suitable host than CBP for guest BZQPG. This ensures that more efficient recombination of holes and electrons occurs at the FPPCA host sites; energy is then more efficiently transferred from host to guest in PIr8. In view of the obvious benefit of FPPCA over CBP as the host, the comparable increased luminance curves of PIr15 and CIr15 (**Figure 5c**) implies that the dependence of device performance on the host

in both of the high-content (15 wt%) devices has been greatly reduced. The dominant emission mechanism is now direct exciton formation on the BZQPG molecules. Hence, an appropriate selection of host and guest material is crucial in improving the EL performance of PHOLEDs.[14] This result using the FPPCA:BZQPG host-guest system is intriguing. Two exciton-formation modes, namely, host-guest energy transfer and direct exciton formation, co-exist to harvest as many excitons as possible for electrophosphorescent emission through adjusting the dopant concentration (8-15 wt%) of BZQPG in FPPCA. By these processes the extraordinarily high and almost constant EL performance in PIr8 and PIr15 is achieved, as shown in **Figure 5** and summarized in **Table 1**.

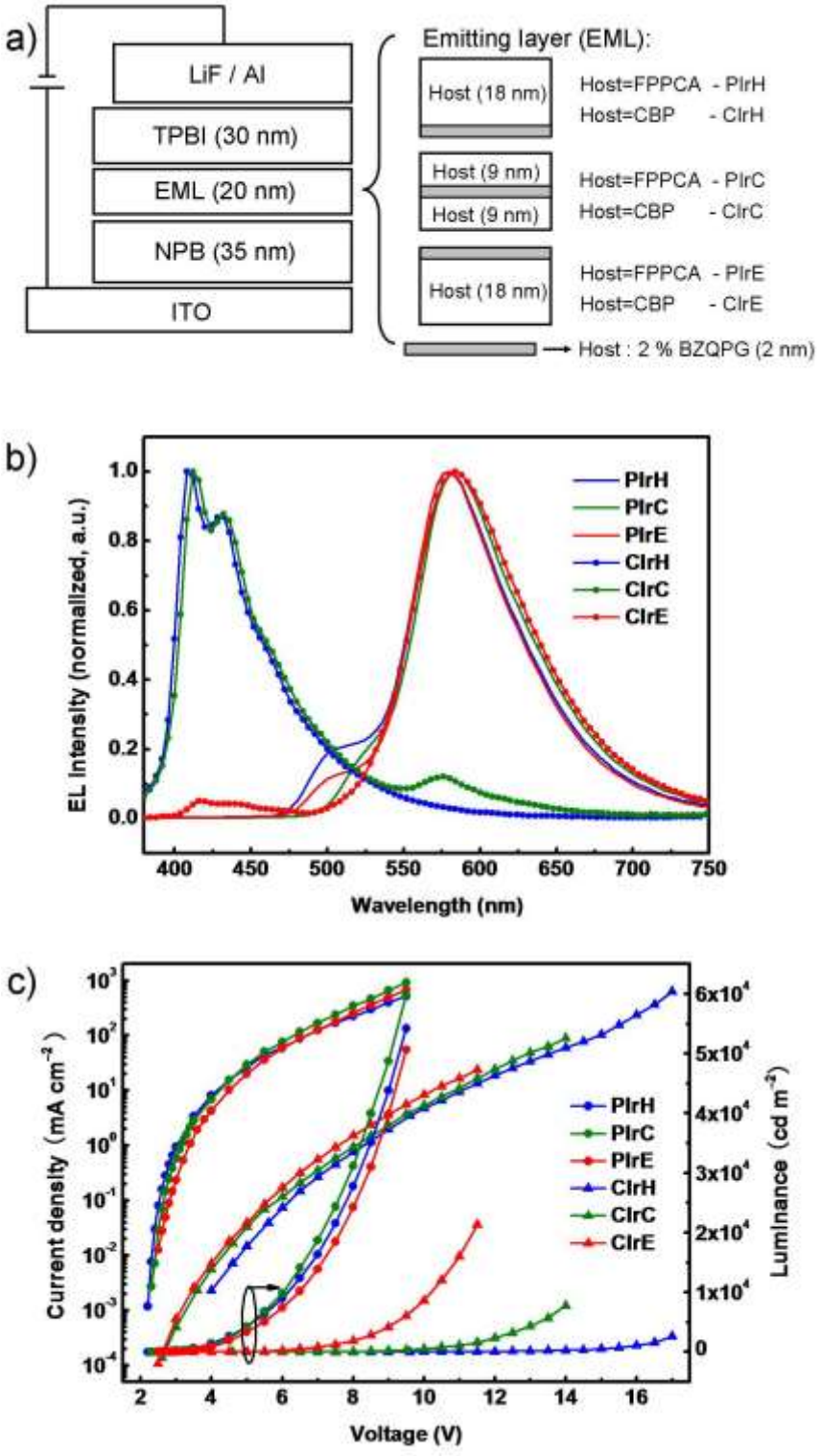

Figure 6. a) Schematic structures of the devices of PIrH, PIrC, PIrE, CIrH, CIrC and CIrE. b) EL spectra of PIrH, PIrC, PIrE, CIrH, CIrC and CIrE at the luminance of 500 cd m^{-2}. c) Current density-voltage-luminance (*J*-*V*-*L*) curves of PIrH, PIrC, PIrE, CIrH, CIrC and CIrE.

To further probe the charge transporting properties of the host phosphor FPPCA and to confirm the recombination zone in the FPPCA-based EMLs, three devices were fabricated by introducing a thin layer (2 nm) of BZQPG doped in FPPCA at a low concentration (2 wt%) into different zones in the EML of PIr100. As shown in **Figure 6a**, the additional doping layer is located either near the HTL (NPB), in the center of the EML or near the ETL (TPBI), namely devices PIrH, PIrC and PIrE (P-series), respectively. By using CBP as the host instead of FPPCA, three directly comparable devices were fabricated, namely CIrH, CIrC and CIrE (C-series). The low-content of BZQPG adopted here ensures that the BZQPG molecules have a minimal effect on the inherent charge transport properties of the neat FPPCA or neat CBP layer. **Figure 6b** shows the EL spectra at a luminance of 500 cd m^{-2}. **Figure 5c** shows the much higher and more rapidly rising current density and luminance levels of the P-series devices, compared to the C-series. This is consistent with the narrower energy gap and the higher charge transporting ability of FPPCA compared to CBP. Furthermore, in contrast with the obvious dependence of the *L*-*V* curve and the EL spectra on the different zone of the doping layer in the C-series, the P-series devices showed almost coincident *L*-*V* curves and similar EL spectra. The spectra show a dominant orange emission attributed to the BZQPG with slight residual green emission from FPPCA. This further demonstrates that both the holes and the electrons can migrate freely and the excitons form not only at the interfaces, but can diffuse evenly throughout the EMLs based on FPPCA host. Thereby device efficiency is enhanced and long lifetime of the devices is expected through reducing exciton/charge accumulation by appropriately selecting the host material.[3a] This is the key point in realizing such high performance in our all-phosphorescent host-guest system.

3. Conclusions

In summary, we have developed an all-phosphor host-guest doping system based on the novel Ir complexes FPPCA and BZQPG. Very high efficiency orange-red PHOLEDs with low driving voltages and extremely low efficiency roll-off have been demonstrated. To the best of our knowledge, the EL efficiency values for our devices are significantly higher than those previously reported for orange devices with similar CIE coordinates.[2c,2j] Moreover, these literature data are for a considerably more complicated EML structure. The FPPCA/BZQPG-based PHOLEDs achieved constantly high EL efficiency with the peak PE and EQE of >75 lm W^{-1} and 26%. This very high and stable EL performance results from the coexistence of two parallel paths to maximize harvesting of the excitons: (i) effective energy transfer from host (FPPCA) to guest (BZQPG) and (ii) direct exciton formation on BZQPG. These paths alternately dominate the electrophosphorescent emission depending on the content of BZQPG in FPPCA (8 or 15 wt%, respectively). Compared with conventional doped PHOLEDs based on a fluorescent host such as CBP, the all-phosphor system removes the charge-injection barrier from the charge-transport process to the EML due to the inherent narrow E_g of phosphorescent materials. Both complexes BZQPG and FPPCA possess high and balanced charge-transport ability. These advantages ensure the balanced charge fluxes with the exciton recombination regions are broadened as wide as the whole EML, which in turn significantly decreases the probability of TTA. PIr15 showed slightly lower EQE and higher roll-off than PIr8. This implies more TTA quenching at the enhanced dopant level in PIr15 than in PIr8. This ideal all-phosphor host-guest doping system produces PHOLEDs with very high efficiency and low efficiency roll-off using a simple device configuration and easily controlled fabrication processes.

Supporting Information

Supporting Information is available from the Wiley Online Library or from the author.

Acknowledgements

G.L., D.Z. and T.P. contributed equally to the work reported in this article.This work was supported by National Basic Research Program of China (973 Program, 2013CB834805), Natural Science Foundation of China (51173064, 91333201, 51203017 and 51373062). The work in Durham was supported by EPSRC.

Received: ((will be filled in by the editorial staff))
Revised: ((will be filled in by the editorial staff))
Published online: ((will be filled in by the editorial staff))

[1] a) H. Sasabe, J.–I. Takamatsu, T. Motoyama, S. Watanabe, G. Wagenblast, N. Langer, O. Molt, E. Fuchs, C. Lennartz, J. Kido, *Adv. Mater.* **2010**, *22*, 5003; b) C.–J. Zheng, J. Wang, J. Ye, M.–F. Lo, X.–K. Liu, M.–K. Fung, X.–H. Zhang, C.–S. Lee, *Adv. Mater.* **2013**, *25*, 2205; c) Y.–L. Chang, S. Yin, Z. Wang, M. G. Helander, J. Qiu, L. Chai, Z. Liu, G. D. Scholes, Z. Lu, *Adv. Funct. Mater.* **2013**, *23*, 705; d) Y. Chen, F. Zhao, Y. Zhao, J. Chen, D. Ma, *Org. Electron.* **2012**, *13*, 2807.

[2] a) R. Wang, D. Liu, H. Ren, T. Zhang, H. Yin, G. Liu, J. Li, *Adv. Mater.* **2011**, *23*, 2823; b) C.–H. Fan, P. Sun, T.–H. Su, C.–H. Cheng, *Adv. Mater.* **2011**, *23*, 2981; c) S. Lee, K.–H. Kim, D. Limbach, Y.–S. Park, J.–J. Kim, *Adv. Funct. Mater.* **2013**, *23*, 4105; d) D. Zhang, L. Duan, Y. Li, H. Li, Z. Bin, D. Zhang, J. Qiao, G. Dong, L. Wang, Y. Qiu, *Adv. Funct. Mater.* **2014**, *24*, 3551; e) Y. –L. Chang, Z. B. Wang, M. G. Helander. J. Qiu, D. P. Puzzo, Z. H. Lu, *Org. Electron.* **2012**, *13*, 925; f) M. Zhu, J. Zou, X. He, C. Yang, H. Wu, C. Zhong, J. Qin, Y. Cao, *Chem. Mater.* **2012**, *24*, 174; g) M. Zhu, J. Zou, S. Hu, C. Li, C. Yang, H. Wu, J. Qin, Y. Cao, *J. Mater. Chem.* **2012**, *22*, 361; h) C. Fan, J. Miao, B. Jiang, C. Yang, Hongbin Wu, J. Qin, Y. Cao, *Org. Electron.* **2013**, *14*, 3392; i) C. Fan, L. Zhu, B. Jiang, Y. Li, F. Zhao, D. Ma, J. Qin, C. Yang, *J. Phys. Chem. C* **2013**, *117*, 19134; j) C. Fan, C. Yang, *Chem. Soc. Rev.* DOI: 10.1039/c4cs00110a.

[3] a) T. Tsuzuki, S. Tokito, *Adv. Mater.* **2007**, *19*, 276; b) Z. Q. Gao, M. Luo, X. H. Sun, H. L. Tam, M. S. Wong, B. X. Mi, P. F. Xia, K. W. Cheah, C. H. Chen, *Adv. Mater.* **2009**, *21*, 688; c) A. Chaskar, H.-F. Chen, K.-T. Wong, *Adv. Mater.* **2011**, *23*, 3876.

[4] T. Peng, Y. Yang, Y. Liu, D. G. Ma, Z. M. Hou, Y. Wang, *Chem. Commun.* **2011**, *47*, 3150.

[5] a) R. J. Holmes, B. W. D'Andrade, S. R. Forrest, X. Ren, J. Li, M. E. Thompson, *Appl. Phys. Lett.* **2003**, *83*, 3818; b) Q. Wang, J. Q. Ding, D. G. Ma, Y. X. Cheng, L. X. Wang, X. B. Jing, F. S. Wang, *Adv. Funct. Mater.* **2009**, *19*, 84; c) H. B. Wu, G. J. Zhou, J. H. Zou, C.–L. Ho, W. –Y. Wong, W. Yang, J. B. Peng, Y. Cao, *Adv. Mater.* **2009**, *21*, 4181.

[6] a) Y. Liu, K. Q. Ye, Y. Fan, W. F. Song, Y. Wang, Z. M. Hou, *Chem. Commun.* **2009**, 3699; b) T. Peng, H. Bi, Y. Liu, Y. Fan, H. Z. Gao, Y. Wang, Z. M. Hou, *J. Mater. Chem.* **2009**, *19*, 8072.

[7] a) Y. C. Zhu, L. Zhou, H. Y. Li, Q. L. Xu, M. Y. Teng, Y. X. Zheng, J. L. Zuo, H. J. Zhang, X. Z. You, *Adv. Mater.* **2011**, *23*, 4041; b) C. Murawski, P. Liehm, K. Leo, M. C. Gather, *Adv. Funct. Mater.* **2014**, *24*, 1117.

[8] a) S. C. Tse, K. C. Kwok, S. K. So, *Appl. Phys. Lett.* **2006**, *89*, 262102; b) K. K. Tsung, S. K. So, *Appl. Phys. Lett.* **2008**, *92*, 103315.

[9] Y. Q. Li, M. K. Fung, Z. Y. Xie, S.-T. Lee, L.-S. Hung, J. M. Shi, *Adv. Mater.* **2002**, *14*, 1317.

[10] a) C. W. Tang, S. A. VanSlyke, C. H. Chen, *J. Appl. Phys.* **1989**, *65*, 3610; b) M. T. Li, W. L. Li, W. M. Su, F. X. Zang, B. Chu, Q. Xin, D. F. Bi, B. Li, T. Z. Yu, *Solid-State Electronics* **2008**, *52*, 121; c) S.-Y. Takizawa, V. A. Montes, P. Anzenbacher, Jr, *Chem. Mater.* **2009**, *21*, 2452.

[11] a) J. Lee, J.–I. Lee, J. Y. Lee, H. Y. Chu, *Org. Electron.* **2009**, *10*, 1529; b) S. L. Gong, Y. H. Chen, J. J. Luo, C. L. Yang, C. Zhong, J. G. Qin, D. G. Ma, *Adv. Funct. Mater.* **2011**, *21*, 1168.

[12] a) T. Peng, G. M. Li, K. Q. Ye, C. G. Wang, S. S. Zhao, Y. Liu, Z. M. Hou, Y. Wang *J. Mater. Chem. C* **2013**, *1*, 2920. b) T. Peng, G. M. Li, K. Q. Ye, S. Huang, Y. Wu, Y. Liu, Y. Wang, *Org. Electron.* **2013**, *14*, 1649.

[13] a) D. Tanaka, H. Sasabe, Y. J. Li, S.–J. Su, T. Takeda, J. Kido, *Jpn. J. Appl. Phys. Part 2* **2007**, *46*, L10; b) S. J. Su, T. Chiba, T. Takeda, J. Kido, *Adv. Mater.* **2008**, *20*, 2125; c) Y. T. Tao, Q. Wang, C. L. Yang, C. Chong, J. G. Qin, D. G. Ma, *Adv. Funct. Mater.* **2010**, *20*, 2923; d) Y.–S. Park, S. Lee, K.–H. Kim, S.–Y. Kim, J.–H. Lee, J.–J. Kim, *Adv. Funct. Mater.* **2013**, *23*, 4914 ; e) K.–H. Kim, C.K. Moon, J.–H. Lee, S.–Y. Kim, J.–J. Kim, *Adv. Mater*. **2014**, *26*, 3844; f) Y. J. Cho, K. S. Yook, J. Y. Lee, *Adv. Mater*. **2014**, *26*, 4050.

[14] W. S. Jeon, T. J. Park, S. Y. Kim, R. Pode, J. Jang, J. H. Kwon, *Org. Electron.* **2009**, *10*, 240.